

# Comparison and Implications of Charge Collection Measurements in Silicon and InGaAs Irradiated by Energetic Protons and Neutrons

E. Normand, D. L. Oberg, J. L. Wert & P.P. Majewski,  
*Boeing Defense & Space Group, Seattle, WA 98124-2499*

G. A. Woffinden, *Amdahl Corp.*

S. Satoh and K. Sasaki, *Fujitsu Laboratory Ltd and Fujitsu Ltd.*

M. G. Tverskoy & V.V. Miroshkin, *Petersburg Nuclear Physics Institute*

N. Goleminov, *Moscow Engineering and Physics Institute*

S. A. Wender and A. Gavron, *Los Alamos National Laboratory*

## Abstract

A variety of charge collection measurements by energetic protons and neutrons have been measured and compared. These include deposition in: small silicon junctions, large volume American and Russian silicon surface barrier detectors, and InGaAs photodiodes.

## INTRODUCTION

A limited number of charge collection measurements using high energy neutrons and protons have been reported [1-4]. Since these measurements can provide insight into the mechanisms for single event upset and latchup by neutrons and protons in microelectronic devices, it is worthwhile compiling and comparing a diverse set of such measurements. Three different types of charge collection measurements will be discussed: a) high energy neutrons in small silicon subvolumes, b) high energy neutrons and protons in large silicon volumes, namely surface barrier detectors (SBDs) and c) high energy neutron in InGaAs photodiodes.

Most of the measurements are new. These include the measurements in the small silicon devices by Fujitsu and in the InGaAs photodiodes. The Russian and American SBD results were previously published [1-4]. However, additional information was obtained relating to the test conditions of the two Russian measurements that enabled the Russian data to be transformed into a different format. This allowed their energy deposition measurements to be directly compared against those obtained from roughly comparable American tests.

All the high energy neutron measurements were made at the Weapons Neutron Research (WNR) facility at the Los Alamos National Laboratory. For the silicon SBD measurements, these will be compared against energy deposition curves measured using several different high energy proton beams, including two in Russia. Thus, these measurements represent energy depositions at four different proton facilities: the Harvard Cyclotron (154 MeV), TRIUMF (200 MeV), the Petersburg Nuclear Physics Institute (PNPI, 1000 MeV) and the Joint Institute for Nuclear Research (JINR) at Dubna, Russia (3650 MeV). The JINR tests were

conducted by Moscow Engineering & Physics Institute (MEPhI) personnel.

The silicon SBDs, both those used by Boeing and Clemson University, as well as those in Russia, appear to be quite similar. The other devices are more unique. The small silicon subvolumes were test devices specially developed by Fujitsu Ltd. and Fujitsu Laboratories Ltd., and were tested by personnel from Amdahl Corporation and the two Fujitsu companies. These devices contained two test structures having the same overall area, one comprised of a single structure and the other of 36,000 small junctions. The InGaAs photodiodes are produced by Epitaxx Corp. Three different sized photodiodes were used, the two larger diameter diodes to increase the charge deposition, and the smaller diode to be typical of those incorporated into fiber optic data bus subsystems.

## SILICON - SMALL VOLUMES

Fujitsu Laboratories and Fujitsu Laboratories Ltd. fabricated chips containing the charge collection test structures. There were two test structures, one a single large structure,  $120\mu\text{m} \times 1200\mu\text{m}$ , and the other an array of 36,000 small structures (each with active area of  $2\mu\text{m} \times 2\mu\text{m}$ ). As shown in Figure 1, the overall active area of each was identical,  $1.44 \text{ E}5 \mu\text{m}^2$ , and each was comprised of the same  $\text{N}^+$  diffusion (depth of  $4\mu\text{m}$ ) structure in a  $\text{P}^+$  well over a  $\text{P}$ -substrate. The array of 36,000 small parallel junctions also had a 10:1 major/minor axis, i.e., were arranged in a  $600 \times 60$  array. Each square-shaped active area was separated from one another by  $1\mu\text{m}$  of the  $\text{p}$  well that served as an isolation barrier. Eight such chips were simultaneously exposed to the high intensity neutron beam of WNR in beamline 30L. Figure 2 shows the energy spectrum of the WNR neutrons. Charge was collected in both structures at 3 and 6 volt bias when the beam was at normal incidence. With the structures at 3V, charge was also collected at incident angles of 0, 30, 60, 90 and 180 degrees.

The measured integral charge collection spectrum from the combined array of small structures is shown in Figure 3 in Burst Generation Rate (BGR) units, [i.e. (number counts depositing  $> E$ )/(volume x fluence)]. Figure 3 shows that for

$E_{dep} \leq 6$  MeV, the variation in the charge collected with the angle of incidence is relatively small (< factor of 2). For energy deposition of  $>6$  MeV, this energy deposition variation with angle of incidence is much more pronounced, and for  $E_{dep} > 10$  MeV, the variation with angle is very large.

is divided by the fluence, normalizes out the total number of counts at each angle, but it doesn't eliminate the poor statistics of low counts for high energies.

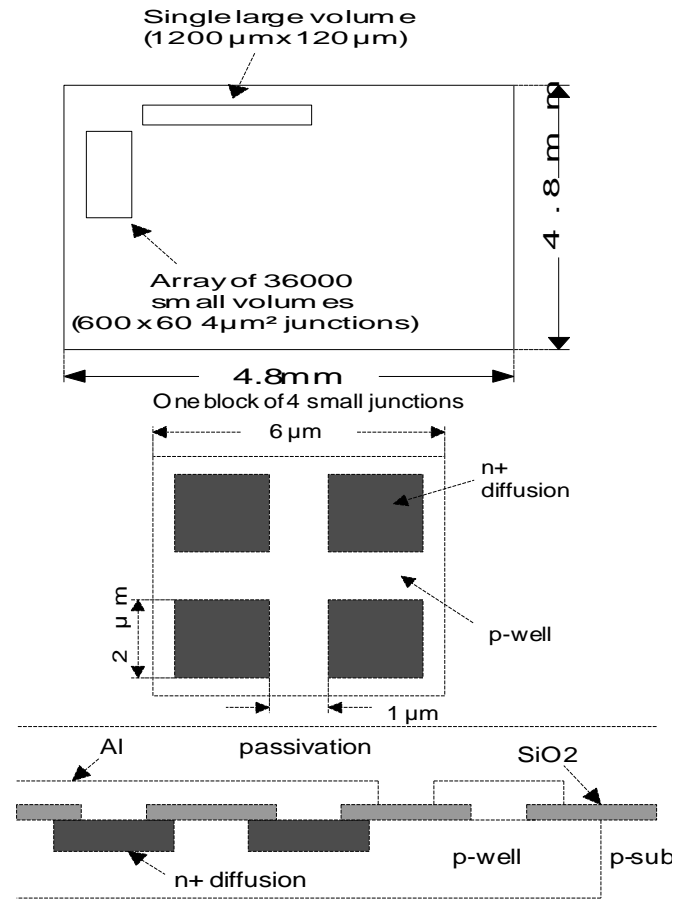


Figure 1 Layout of Chip with Silicon Test Structures, Single Large Volume and Array of Small Subvolumes

deposition at 10 MeV represents a small fraction of the total deposition, and is based on a very small number of counts. Figure 4 contains a similar comparison of the measured energy deposition in the single large volume of active silicon. Again, the energy deposition curves are quite similar for  $E_{dep} \sim 5$  MeV, and exhibit very large differences for  $E_{dep} > 8$  MeV.

The test devices acquired fluences that ranged between  $3-6 \times 10^{10}$  n/cm<sup>2</sup> during each run (combination of applied voltage and device orientation to the beam). Thus a large number of depositions were recorded during each run, roughly  $1 \times 10^4$ , spread over a very fine deposition structure of approximately 1000 channels (0.01-15 MeV, 0.0156 MeV/channel), although only the lowest 400 channels received many counts. For the single large structure data of Fig. 4, > 99.5% of these counts were for energy depositions of  $< 6$  MeV. Thus for  $E_{dep} > 6$  MeV statistical uncertainties make it difficult to discern from Fig. 3 whether there is an actual trend in the data regarding the variation of deposition rate with angle of incidence. The BGR format, in which the number of counts

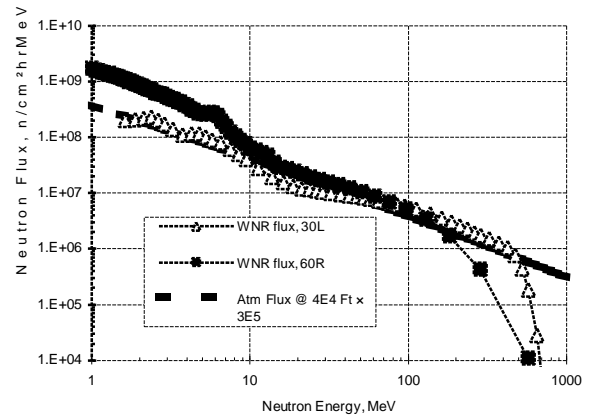


Figure 2 Energy Spectrum of the WNR Neutron Beam (30L) Used for Charge Collection Measurements

To assess the statistical uncertainties, a closer evaluation of the actual number of counts in the single large structure used in constructing Fig. 4 is tabulated in Table 1. To make the comparison more consistent between the runs, the number of counts in each run has been normalized to  $1 \times 10^4$  counts (similar to normalizing by fluence). Statistical uncertainties for each normalized number of counts is taken as  $\sqrt{\text{counts}}$ . As seen in Table 1, for  $E_{dep} > 4$  MeV and 3V operation, the

Table 1 Energy Deposition Counts for Large  $E_{dep}$  by WNR Neutrons in Large Silicon Subvolume

	Angle of Incidence				
	3V, 0°	3V, 30°	3V, 60°	3V, 90°	3V, 180°
Number of Counts					
Total Cnts > 0.02 MeV	14,056	8,337	10,062	9,388	6,906
Actual Cnts > 4MeV	210	158	201	175	103
Norm'lzd Cnts > 4MeV	149 ±12	190 ±14	200 ±14	186 ±14	149 ±12
Actual Cnts > 6MeV	47	23	38	37	16
Norm'lzd Cnts > 6MeV	33 ± 5.7	28 ± 5.3	38 ± 6.2	39 ± 6.2	23 ± 4.8
Actual Cnts > 8MeV	10	6	8	17	4
Norm'lzd Cnts > 8MeV	7 ± 2.6	7 ± 2.6	8 ± 2.8	18 ± 4.2	6 ± 2.4
Actual Cnts > 10MeV	0	0	0	5	0
Norm'lzd Cnts > 10MeV	0	0	0	5 ± 2.2	0

normalized number of counts varied from  $149 \pm 12$  to  $200 \pm 14$  over the five different angles of incidence, indicating fair uniformity over all angles of incidence. However for  $E_{dep} > 8$  MeV, the normalized number of counts was  $18 \pm 4.2$  at  $90^\circ$

incidence, but varied between  $6-8 \pm 2.7$  for the other four angles of incidence. This same trend of much larger deposition at  $90^\circ$  is even more apparent in the data for  $E_{dep} > 10$  MeV, where at  $90^\circ$  incidence there were  $5 \pm 2.2$  counts, recorded but none at the other angles of incidence.

Even accounting for the poor statistics, it appears that the neutrons striking at  $90^\circ$  (grazing incidence) produce significantly more high energy deposition than at normal or near-normal angles of incidence. It appears that this is due to

deposition from the secondary protons and alpha particles. For grazing angles, these light secondary particles, generally emitted in the forward direction, will be facing much longer paths (minimum of  $120 \mu\text{m}$ ) over which to deposit appreciable energy compared to the normal incidence case of  $\sim 4 \mu\text{m}$  path length (approximate diffusion depth). This same angular dependence effect (peaking of high energy deposition at  $90^\circ$ ) was also seen in charge collection measurements with 300 MeV protons [14].

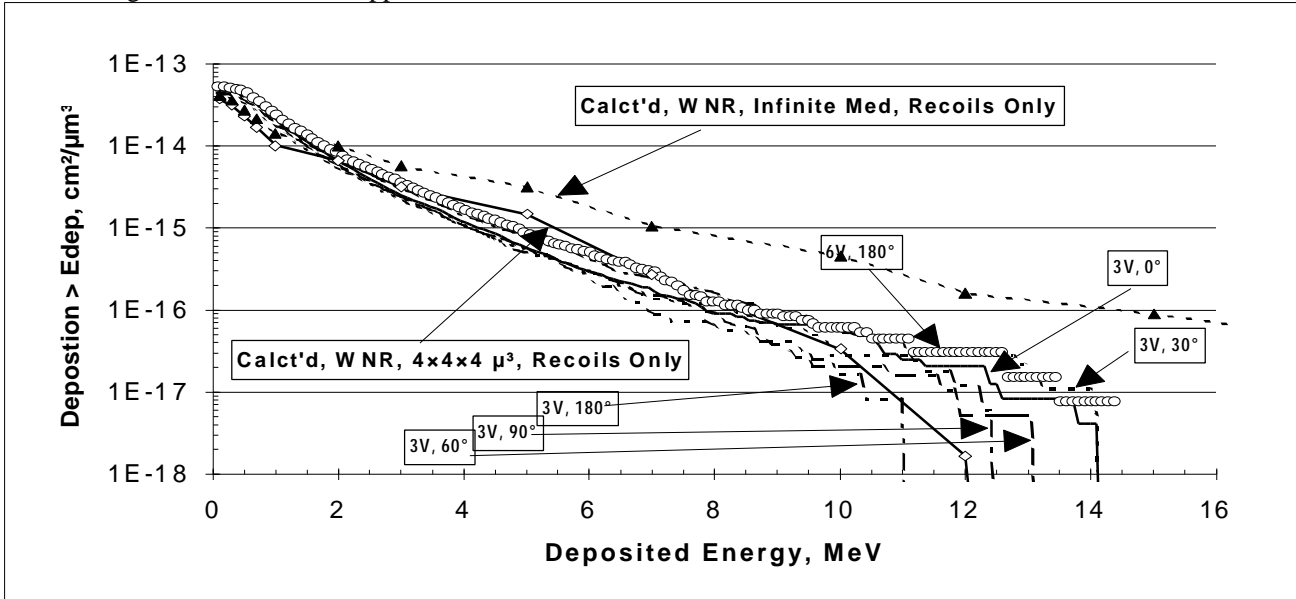


Figure 3 Energy Deposition Curves for Array of Small Silicon Subvolumes in WNR Beam at Various Angles of Incidence

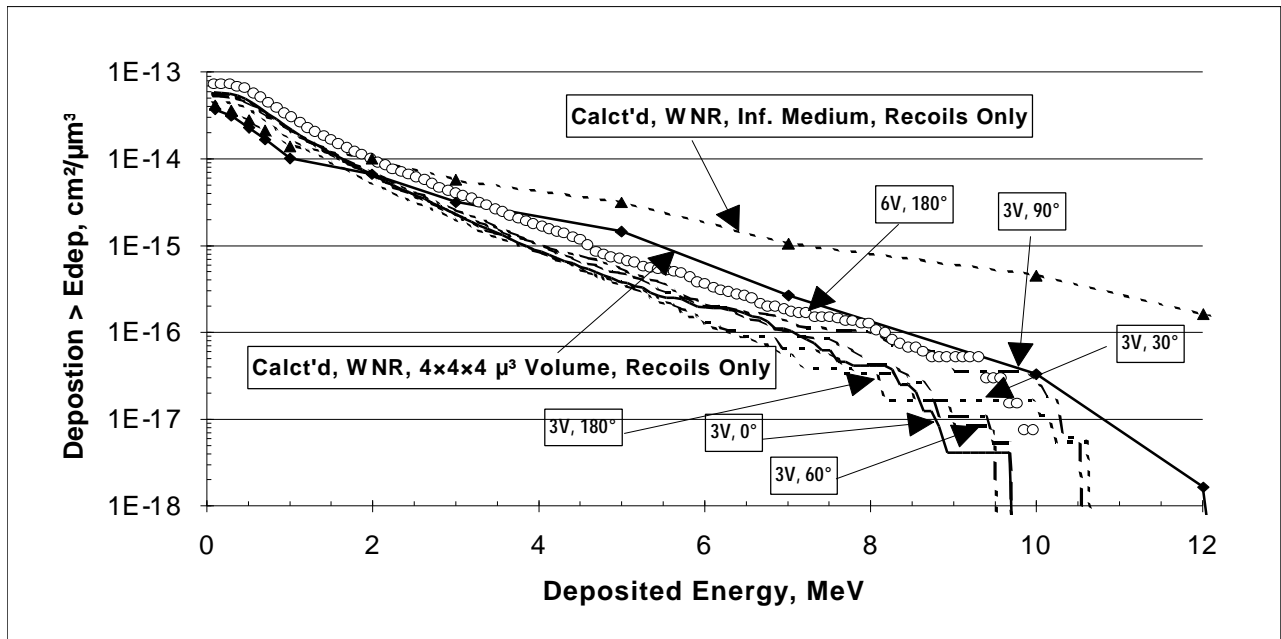


Figure 4 Energy Deposition Curves for Single Large Volume in WNR Neutron Beam at Various Angles of Incidence

In Figs. 3 and 4 we also compare calculated values of the BGR deposition by high energy neutrons obtained from the Los Alamos version of the HETC code, LAHET [8]. Unfortunately, LAHET calculations are available for only a

limited number of models [9], and none is fully applicable to the test structure geometry and deposition conditions. The closest calculation is for that of a  $4 \times 4 \times 4 \mu\text{m}^3$  volume of silicon that only accounts for the energy deposited by the recoils, and a similar calculation based on an infinite medium of silicon. The WNR neutron spectrum is very similar to that of the atmospheric neutrons, having the property that about 1/3 of the neutrons are in each of the three energy ranges: 1-10 MeV, 10-100 MeV and 100-700 MeV. The calculated BGR energy deposition curves for the WNR spectrum that are in Figs 2 and 3 are based on averaging the BGR functions for neutrons of three different energies, 8 [10], 50 and 200 MeV [9], each being representative of one of the three aforementioned broad energy ranges with a nearly equal number of neutrons.

Overall, energy deposition by the recoils in the  $4 \times 4 \times 4 \mu\text{m}^3$  volume is much more representative of deposition in the test structures than are the recoils in the infinite medium calculation, although for  $E_{\text{dep}} < 5$  MeV the deposition is relatively similar for the two geometries. For  $E_{\text{dep}} > 5$  MeV, energy deposition in the infinite medium far exceeds that measured in the test structures as seen in Figs. 2 and 3. Out to about  $E_{\text{dep}} \sim 10$  MeV, the calculated energy deposition in the  $4 \times 4 \times 4 \mu\text{m}^3$  volume is in relatively good agreement with the measured curves, but for  $E_{\text{dep}} > 10$  MeV, the calculated deposition falls off far too rapidly. This is due to the energy deposition from the light reaction products, i.e., protons and alpha particles, which isn't included in the LAHET calculations. The role of the protons is further discussed below in order to explain other aspects of the measured deposition.

In Fig. 5 we directly compare the measured energy deposition in the array of small volumes with that in the single large volume. From Fig. 5 it is clear that for  $E_{\text{dep}} > 5$  MeV the deposition is greater in the array than in the single volume. There appear to be at least two factors that account for this: a) the effective junction is actually larger in the array due to the additional sidewall junctions between the N+ subvolumes and the surrounding P-well, allowing for additional charge collection, and b) enhanced deposition due to the additional energy degradation in the secondary protons. Energy deposited by protons and alpha particles, which have long ranges compared to the ranges of the neutron-induced recoils ( $< 8 \mu\text{m}$ ), plays a very important role. The increased energy deposition in the array is partially due to the protons and alpha particles and their energy degradation through the extra silicon isolating each small subvolume. The cumulative effect of the extra silicon surrounding each subvolume is to degrade the energy of the protons further than in the single large volume. Because the  $dE/dx$  of the protons and alpha particles increases as the energy decreases (for  $E > 1$  MeV), the net result is that the energy deposition is increased.

This can be more clearly shown by example, taking a neutron interaction resulting in the production of an energetic

proton, (in this case 15 MeV), that is assumed to occur at the center of the volume of active silicon. For a simple  $90^\circ$  scattering, the longest path length through the entire volume is along the major axis; for the single volume it is  $600 \mu\text{m}$ , but for the array, it is  $900 \mu\text{m}$  (cumulatively  $600 \mu\text{m}$  of active silicon and  $300 \mu\text{m}$  of isolating p-silicon). In the single large volume, the energy deposition over the last  $2 \mu\text{m}$  of active silicon is  $0.015$  MeV, and over the last  $10 \mu\text{m}$  of active silicon, it is  $0.074$  MeV. By comparison, in the array of small subvolumes the energy deposition over the last  $2 \mu\text{m}$  of active

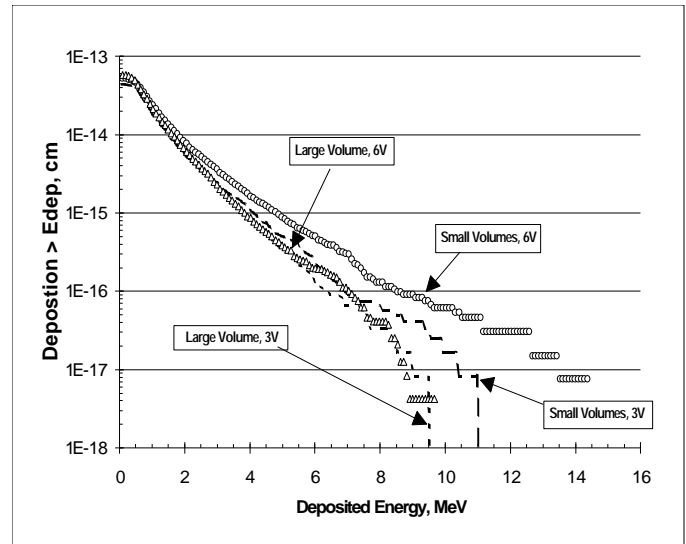


Figure 5 Comparison of Charge Collection in Large and Small Test Structures in WNR Beam at Normal Incidence

silicon is  $0.018$  MeV, and over the last  $10 \mu\text{m}$  of active silicon, it is  $0.090$  MeV. Thus near the outer edge of the active volumes, approximately 20% more energy is deposited by a 15 MeV proton in the active portion of the array of subvolumes compared to that in the single large volume due to the increased  $dE/dx$  of the lower energy protons. This 20% increase is consistent with the increased energy deposition overall seen in Fig. 5.

A similar argument could also be made for energy deposition by alpha particles, but in this case, because the range of alpha particles is much smaller than that of protons, the energy deposition would have to be along the minor axis. For large active volumes of silicon, this key role in the overall energy deposition played by the light reaction products rather than the recoils was earlier investigated via measurements of energy deposition by 14 MeV neutrons impinging on a large volume silicon SBD [11]. For the 14 MeV neutrons, calculations showed that it was the energy deposition from alpha particles that was the dominant factor.

With the WNR beam it appears that it is the protons that are primarily responsible. A further verification of this can also be found by examining Table 1 and Figs. 3 and 4, and comparing the energy deposition curves for the virtually identical configurations of 3V,  $0^\circ$  and 3V,  $180^\circ$  in each

figure. The beam-device orientation is the same, in one case the beam strikes the front of the device, in the other case, the back. Looking at the two figures, energy deposition for  $E_{dep} < 5$  MeV is identical, small differences show up for  $8 \text{ MeV} < E_{dep} < 5 \text{ MeV}$ , and larger differences for  $E_{dep} > 8 \text{ MeV}$ . Considering the very short range of the recoils of  $< 10 \text{ MeV}$  ( $< 10 \text{ }\mu\text{m}$ ), especially in the single large volume, it is clear that the recoils within the active volume should produce the same energy deposition in the device whether it is struck from the front or the back. Therefore, it must be the light reaction products with long ranges, protons and alpha particles, that are responsible for the differences in energy deposition. Finally, Fig. 5 shows that energy deposition is greater at 6V bias than at 3V, and the reason for this is the increased depletion depth a the higher voltage.

### SILICON - LARGE VOLUMES (SBDs)

A limited number of charge collection measurements in SBDs by high energy protons have been reported, most by McNulty and co-workers [1]. All these were at the Harvard Cyclotron and used SBDs with several different thicknesses of collection depth. Boeing made independent measurements with high energy protons (TRIUMF) and the WNR neutron beam at Los Alamos using SBDs with 10 and 300  $\mu\text{m}$  thickness [2].

Similar measurements were carried out in Russia [3,4]. At the Petersburg Nuclear Physics Institute (PNPI) the energy deposited by a narrow 1 GeV beam of protons (fluence of  $4E10 \text{ p/cm}^2$ ) in a 20  $\mu\text{m}$  thick SBD was measured. The differential energy deposition reported in [3] was converted to the integral deposition in the BGR format. In addition, a

larger and thicker SBD, 86  $\mu\text{m}$ , was used by MEPhI personnel and exposed to the 3.65 GeV proton beam (fluence of  $3.8E5 \text{ p/cm}^2$ ) at the JINR beam in Dubna, Russia and the energy deposition was measured [4]. This energy deposition was also converted to the BGR format. In Figure 6 we plot the charge deposition curves measured by these four groups: the McNulty group [1], Boeing [2], PNPI [3] and MEPhI [4] for SBDs of various thicknesses. The energy deposition curves appear to fall into three families that mainly depend on the thickness of the SBD: very thin (10  $\mu\text{m}$ ), thin (20-25  $\mu\text{m}$ ) and thick (90-300  $\mu\text{m}$ ). The PNPI 20  $\mu\text{m}$  SBD in a 1 GeV proton beam has a similar energy deposition curve as El-Teatey's 25  $\mu\text{m}$  detector with 154 MeV protons. Similarly, energy deposition in the MEPhI 90  $\mu\text{m}$  detector by 3.65 GeV protons matches that of the WNR neutron beam (upper energy of  $\sim 700 \text{ MeV}$ ) in the 300  $\mu\text{m}$  detector. It thus appears that the thickness of the SBD is a more important factor than the

**Table 2 Characteristics of Various Proton/Neutron SBD Energy Deposition Measurements Shown in Figure 6**

Particle	Part'le Energy MeV	SBD Thick $\mu\text{m}$	Symb in Fig. 6	Org. or Author	Ref .
Proton	1000	20	*	PNPI	3
Proton	154	25	□	El-Teatey	1
Proton	154	10	△	El-Teatey	1
Neutron	<700	10	●	Boeing	2
Neutron	<700	300	▲	Boeing	2
Proton	3600	90	+	MEPhI	4

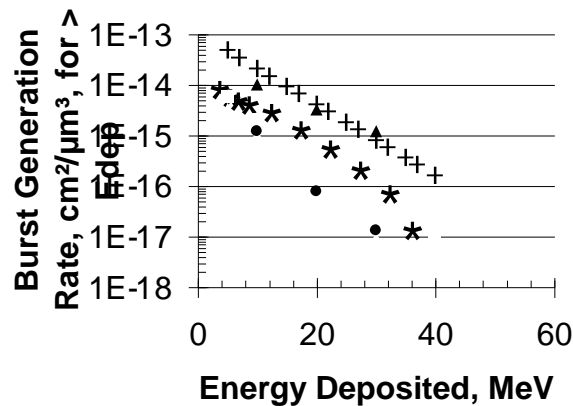


Figure 6 Comparison of Energy Deposition in Silicon SBDs from High Energy Protons and Neutrons energy of the particles in determining the energy deposition. This is discussed in greater detail in the section on energy deposition in InGaAs where the role of secondary protons, which also applies to silicon SBDs, is elaborated upon.

### INGAAS PHOTODIODES

Photodiodes are used within the receiver portion of fiber optic data systems, and their sensitivity to ionizing radiation, in particular to single event effects (SEE) [5,6] has been shown. Both Si and InGaAs photodiodes have been used, but InGaAs has been identified as less prone to SEE because a

minimal depletion depth,  $\sim 2\mu\text{m}$ , can be used and still achieve a high quantum efficiency. SEE testing of fiber optic systems has shown the PIN photodiode to be one of the most sensitive components [5]. The photodiodes have been tested with proton beams and measured in terms of the induced bit error rate [5,6]. In addition, calculated NIEL (non ionizing energy loss) for protons impinging on InGaAs have shown excellent correlation with measured generation lifetime damage factors in InGaAs [6,7]. Since the bit error rate has been observed to increase with decreasing proton energy, the main mechanism identified is that of direct ionization energy loss rather than proton-induced nuclear interaction [6,7]. Although all measurements in the photodiodes have been consistent in highlighting the important role of direct ionization, no tests had previously been performed with a InGaAs photodiode in a neutron beam to directly measure the nuclear interaction contribution.

Since the WNR neutron beam is the most energetic and intense neutron beam available, it was used to directly measure the sensitivity of InGaAs photodiodes to nuclear induced effects. Three different Epitaxx InGaAs photodiodes, those with diameters of 3000, 1000 and 75  $\mu\text{m}$ , were irradiated in the WNR beam and the energy deposition curves were recorded. The larger diameter photodiodes are relatively similar in size to the silicon SBDs discussed above, and its energy deposition curve will be discussed below.

From a systems standpoint, perhaps the most important parameter is the average fluence of neutrons needed to induce a single, measurable pulse in the InGaAs photodiode. The summary data from our charge collection measurements are tabulated in Table 3. This data shows that in a high energy neutron field, a neutron fluence of between  $1\text{E}5\text{-}1\text{E}8\text{ n/cm}^2$  is needed to generate a single measurable pulse ( $>0.5\text{ MeV}$ ). By comparison, Marshall et al [12] found through bit error rate (BER) testing of the 75  $\mu\text{m}$  photodiode with 63 MeV protons, that the nuclear component required about  $1\text{E}4\text{ particles/cm}^2$ . The difference is attributable to different interaction probabilities between the two beams (monoenergetic protons and WNR neutrons), and to a greater sensitivity on the part of the BER test scheme compared to our direct measurement of energy deposition in the photodiode. Regardless of which measure of the nuclear component applies, it is in sharp contrast to the situation in a high energy proton field in which essentially every particle leads to a BER pulse [6]. This verifies by direct measurement that the nuclear-induced effect in InGaAs is small.

**Table 3 Energy Deposition in InGaAs Photodiodes by WNR Neutrons**

Photodiode Diameter, $\mu\text{m}$	WNR Fluence $\text{n/cm}^2$	Pulses	Fluence per pulse
75	1.8E11	2.2E3	8E7
1000	2.6E10	2.4E4	1E6

3000	2.1E10	9.5E4	2E5
------	--------	-------	-----

## ENERGY DEPOSITION IN THE INGAAS PHOTODIODES

In Figure 7 are shown the energy deposition curves from the two largest InGaAs photodiodes. These represent the first charge collection measurements in InGaAs by neutral particles that we are aware of, and so there is some uncertainty in interpreting this data. The two photodiodes, with optical diameters of 1 mm and 3 mm are believed to have very similar depletion depths,  $\sim 5\mu\text{m}$ , so they both have volumes that are in the shape of a very thin pancake. The difference in the volumes, a factor of 9, is due solely to the differences in the diameters.

For consistency with previous measurements discussed in this paper the energy deposition curves in Fig.7 are displayed in the BGR format, however in this case it appears that the BGR format may be misleading. On a per volume basis the smaller photodiode appears to have greater capability of absorbing energy than the larger one. There are two reasons for this is: a) the depletion depth is probably different for the two photodiodes and b) most of the energy collected by the photodiode is deposited by the light reaction products,

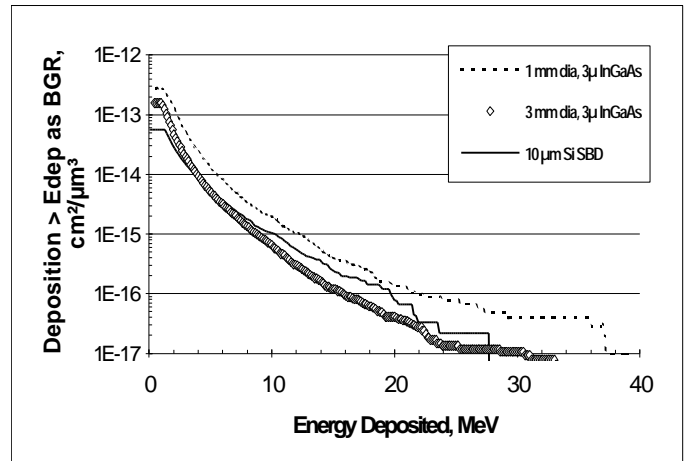


Figure 7 Energy deposition in Two InGaAs Photodiodes in WNR Neutron Beam

primarily protons but also alpha particles, and not by the heavier recoils. We are uncertain of the depletion depth of the photodiodes and so assumed that it is the same in both devices, 5  $\mu\text{m}$ . However, since the manufacturer recommends that they be operated at different biases (5V for the 1 mm diode and 1V for the 3 mm diode), in fact, the depletion depth very likely is different for each of the photodiodes, but probably within a factor of 2 for the two devices.

Secondly, regarding energy deposition by the recoils, it is very localized because the range of the recoils is very short, e.g., a 5 MeV Cu in InGaAs has a range of  $\sim 2\mu\text{m}$ . Energy from the protons is deposited over a much longer path length. Based on use of the TRIM code [13], in InGaAs, the range of a 10 MeV proton is  $\sim 450\mu\text{m}$  and is  $\sim 250\mu\text{m}$  for a 7 MeV

proton so a long path length within the photodiode is needed to capture all the proton energy. Thus the outer 0.5 mm annulus of the larger photodiode, even though it comprises ~30% of the total volume of the device, will receive only a small fraction of the energy of the secondary protons for  $E_p > 10$  MeV that are created in this region by neutron interactions.

Assuming the depletion depth to be identical, the nine-fold increase in volume between the two photodiodes is accomplished by increasing the radius from 0.5 to 1.5 mm. However, if we consider the radius as the most representative path length, increasing the path length from 0.5 to 1.5 mm only increases the energy of protons available to deposit significant energy from 11 to 21 MeV. Alternately, by considering the diameter as the maximum path length, the maximum proton energy available for deposition is increased from 17 MeV (1 mm) to 32 MeV (3 mm). These maximum proton energy depositions are consistent with the two energy deposition curves in Fig. 7. In effect, for thin depletion volumes, increasing the diameter is not as effective in increasing the energy deposition as increasing the thickness, as was previously shown for the silicon SBDs. Therefore expressing the energy deposition on a per volume basis may appear to give misleading results.

We do not have available energy deposition calculations by HETC in InGaAs that could quantify these effects, but such calculations are available for a similar volume of silicon (SBD). In Fig.8 we plot one measured and two calculated energy deposition curves for a 5mm diameter, 10  $\mu\text{m}$  thin silicon SBD in the WNR beam. Two calculations were carried out with LAHET [9], one for the precise dimensions of the SBD that also included the contributions of the light reaction products. The other calculation is for an infinite medium of silicon but includes deposition for only heavy recoils ( $Z > 2$ ). The calculated curve that includes the proton and alpha particle contributions is in very good agreement with the measured energy deposition over the deposition range of 3-23 MeV. In this same energy deposition region the calculation based on only the heavy recoils is low by about a factor of 3. The low energy ( $< 3$  MeV) discrepancy is attributable to the contributions by the 1/3 of all the WNR neutrons with energies  $< 10$  MeV whose effectiveness in the calculation is modeled rather poorly by the lowest energy available in LAHET, 50 MeV. These low energy neutrons make significant contributions only for low energy depositions (e.g., the maximum products of an 8 MeV neutron in silicon are a 4 MeV proton or 5 MeV alpha).

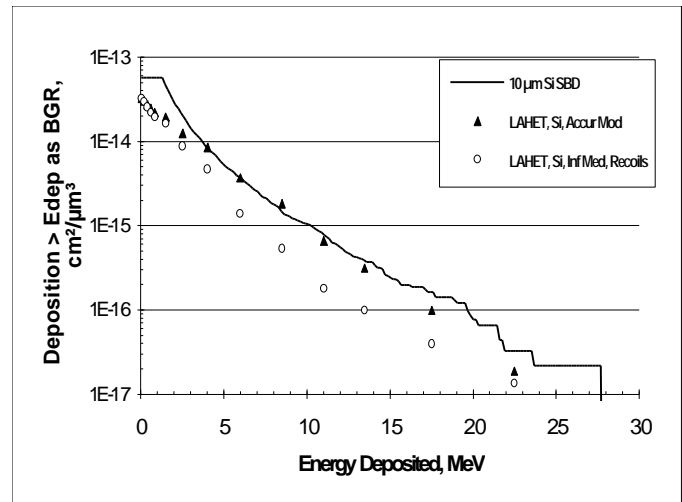


Figure 8 Comparison of Measured and Calculated Energy Deposition in Silicon SBD in WNR Beam

Thus even in silicon, for a very thin but wide volume, most of the energy deposition is from the secondary protons. In InGaAs the importance of energy deposition by the protons is expected to be even greater than in silicon because the photodiode is even thinner than the SBD, the proton range is shorter and the proton  $dE/dx$  is greater (both by factors of about 1.6 compared to silicon). Thus while the BGR format is usually effective in displaying energy deposition, this generally applies when localized deposition by the recoils dominates. Energy deposition in these photodiodes is unusual because they are differentiated by variations in the diameter of the devices, whereas with silicon SBDs, energy deposition has previously been measured in devices of the same diameter but with the thickness being varied.

## CONCLUSIONS

A variety of charge collection measurements have been compiled and compared in three different types of devices: a) small silicon volumes, b) large silicon volumes and c) InGaAs photodiodes. The measurements in the small silicon volumes and the InGaAs photodiodes are new. While the Russian measurements in silicon SBDs aren't new, additional information beyond that in the original publications was obtained from the authors that allowed the depositions to be transformed into the BGR format. This enabled a direct comparison to be made between these Russian measurements, and similar results from American charge collection experiments. This is the first such comparison of charge collection in comparable Western and Russian devices that we are aware of. There are no such instances of SEU measurements in Russian-made RAMs to compare against the many SEU tests in Western RAMs, but this is the first step in that direction.

Small silicon junction devices built by Fujitsu allowed fine detail in the energy deposition spectrum to be measured. In the small silicon junctions, deposition for  $E_{dep} < 6$  MeV, showed limited variation with angle of incidence. For  $E_{dep} >$

8 MeV the largest deposition appeared to occur at grazing incidence, in agreement with proton results and interaction geometries. At higher energy deposition, the array of small subvolumes collected more energy than the single volume of equal size, and this was explained in terms of the increased charge collection through the sidewall junctions and the enhanced secondary proton deposition.

Comparison of the deposition in large volume silicon SBDs, in the US and Russia, showed good agreement, with the SBD thickness appearing to be more important than the particle energy due to the key role played by the secondary protons.

The deposition in the InGaAs photodiodes by energetic neutrons complements previous proton measurements. It is noteworthy because it is the first direct measurement of the nuclear contribution to energy deposition in this material. Energy deposition in the very thin InGaAs photodiodes may appear unusual because these devices are differentiated by variations in the diameter, whereas with silicon SBDs, energy deposition has previously been measured in devices of the same diameter, with the thickness being varied. Based on these results shown in Fig. 7, it would be interesting to carry out new energy deposition measurements in silicon SBDs, using devices with the same depletion depth but varying diameters, to observe how the deposition would vary.

#### ACKNOWLEDGMENT

We gratefully acknowledge the assistance provided by the following people in facilitating, preparing for and carrying out the new tests reported on in this work: J. E. Sunde and C. E. Vick of the Boeing Radiation Effects Laboratory, G. Dutcher of Boeing Defense & Space Group, M. Berninger of LANL, Hiep Le of Amdahl Corp., K. Shono and H. Kikuchi of Fujitsu, Ltd., N. Nakayama of Fujitsu Laboratory Ltd., and P. W. Marshall of NRL.

#### REFERENCES

1. S. El-Teaty, et al "Soft Fails in Microelectronic Circuits Due to Proton-Induced Nuclear Reactions in Material Surrounding the SEU-Sensitive Volume", Nucl. Inst. Methods, **B40**, 1300 (1989)
2. E. Normand, et al, "Single Event Upset and Charge Collection Measurements Using High Energy Protons and Neutrons", IEEE Trans. Nucl. Sci., **41**, 2203 (1994)
3. I. B. Vodopianov, et al. "Energy Deposition Spectra from Nuclear Reactions in Thin Silicon Surface Barrier Detectors Irradiated by 1 GeV Protons", Leningrad Nuclear Physics Institute Preprint N1593 (1990)
4. V. S. Barashenkov, et al, "Peculiarities of the Energy Loss Spectrum of High Energy Particles Penetrating Thin Silicon Plates" Nucl. Inst. Methods, **B58**, 157 (1991)
5. P. W. Marshall, et al "Physical Interactions Between Charged Particles and Optoelectronic Devices and Their

- Effects on Fiber Optic Data Links" Proc. SPIE, **53**, 104 (1993)
6. P. W. Marshall et al "Survivable Fiber Based Data Links for Satellite Radiation Environments" SPIE Critical Review-14, Fiber Optics Reliability and Testing, 1994
7. P. W. Marshall, et al, IEEE Trans. Nucl. Sci., **39**, 1982 (1992)
8. R. E. Prael and H. Lichtenstein, "Users Guide to LCS: the LAHET Code System", LA-UR-89-3014, Los Alamos National Lab, 1989
9. A. Gavron, personnel communication
10. E. Normand and W. R. Doherty, "Incorporation of ENDF-V Neutron Cross Section Data for Calculating Neutron-Induced Single Event Upsets," IEEE Trans. Nucl. Sci., **NS-36**, 2349 (1989)
11. E. Normand et al, "Quantitative Comparison of Single Event Upsets Induced by Protons and Neutrons", IEEE Trans. Nucl. Sci., **38**, 1457, (1991)
12. P. W. Marshall et al "Particle-Induced Bit Errors in High Performance Fiber Optic Data Links for Satellite Data Management" IEEE Trans. Nucl. Sci., **41**, 1958 (1994)
13. J. Biersack and J. Ziegler, TRIM-92 Code, 1992
14. J. Levinson et al, "On the Angular Dependence of Proton Induced Events and Charge Collection", IEEE Trans. Nucl. Sci., **41**, 2098, (1994)



In future, should be on Boeing letterhead, with memo #

February 4, 1995

*Charge Collection Paper*

Dr. Peter McNulty  
IEEE/NSREC Technical Chairman  
Clemson University, Dept. of Physics & Astronomy  
117 Kinard Laboratory of Physics  
Clemson SC 29634-1911

Dear Dr. McNulty:

Please accept the enclosed paper summary for consideration for the 1995 IEEE Nuclear and Space Radiation Effects Conference. We believe that it belongs in the "Single Event Charge Collection Phenomena" session. We may be reached at:

<u>Eugene Normand</u>	Boeing Defense & Space Group P.O. Box 3999, MS 2T-50 Seattle, WA 98124 Phone (206) 544-5626 FAX (206) 544-5438
Other Boeing Personnel	Same Address and FAX as above
Dennis L. Oberg	Phone (206) 544-5400
Jerry L. Wert	Phone (206) 544-5506
Peter P. Majewski	Phone (206) 544-5390
Steven A. Wender	Los Alamos National Laboratory P-17, MS H803 Los Alamos, NM 87545 Phone (505) 667-1344 FAX (505) 665-4121
Avigdor Gavron	Same Address and FAX as above Phone (505) 667-4992

Thank you kindly,

Eugene Normand

In future, should be on Boeing letterhead, with memo #

February 4, 1995

*Upset/Latchup Paper*

Dr. Peter McNulty  
IEEE/NSREC Technical Chairman  
Clemson University, Dept. of Physics & Astronomy  
117 Kinard Laboratory of Physics  
Clemson SC 29634-1911

Dear Dr. McNulty:

Please accept the enclosed paper summary for consideration for the 1995 IEEE Nuclear and Space Radiation Effects Conference. We believe that it belongs in the "Single Event Phenomena in Devices and Circuits" session. We may be reached at:

<u>Eugene Normand</u>	Boeing Defense & Space Group P.O. Box 3999, MS 2T-50 Seattle, WA 98124 Phone (206) 544-5626 FAX (206) 544-5438
Other Boeing Personnel	Same Address and FAX as above
Jerry L. Wert	Phone (206) 544-5506
Peter P. Majewski	Phone (206) 544-5390
William G. Bartholet	P.O. Box 3999, MS 9F-51 Phone: (206) 657-6298
Steven A. Wender	Los Alamos National Laboratory P-17, MS H803 Los Alamos, NM 87545 Phone (505) 667-1344 FAX (505) 665-4121

Thank you kindly,

Eugene Normand

In future, should be on Boeing letterhead, with memo #

February 4, 1995

*MACREE Paper*

Dr. Peter McNulty

IEEE/NSREC Technical Chairman  
Clemson University, Dept. of Physics & Astronomy  
117 Kinard Laboratory of Physics  
Clemson SC 29634-1911

Dear Dr. McNulty:

Please accept the enclosed paper summary for consideration for the 1995 IEEE Nuclear and Space Radiation Effects Conference. We believe that it belongs in the "Modeling of Space Radiation Environments" session. We may be reached at:

<u>Peter P. Majewski</u>	Boeing Defense & Space Group P.O. Box 3999, MS 2T-50 Seattle, WA 98124 Phone (206) 544-5390 FAX (206) 544-5438
--------------------------	--

Other Boeing Personnel	Same Address and FAX as above
------------------------	-------------------------------

Eugene Normand	Phone: (206) 544-5626
Dennis L. Oberg	Phone (206) 544-5400

Thank you kindly,

Peter P. Majewski

# Comparison of Charge Collection Measurements in Silicon and InGaAs Irradiated by Energetic Protons and Neutrons

E. Normand, D. L. Oberg, J. L. Wert & P.P. Majewski, Boeing D&SG  
G. A. Woffinden, Amdahl Corp.  
S. Satoh and K. Sasaki, Fujitsu Laboratory Ltd and Fujitsu Ltd.  
M. G. Tverskoy & V.V. Miroshkin, Petersburg Nuclear Physics Institute  
N. Goleminov, Moscow Engineering & Physics Institute  
S. A. Wender and A. Gavron, Los Alamos National Laboratory

## Abstract

A variety of charge collection measurements by energetic protons and neutrons have been made and compared. These include deposition in: small volume silicon junctions, large volume American and Russian silicon surface barrier detectors, and InGaAs photodiodes. The neutron irradiations were performed at the WNR beam of Los Alamos National Laboratory, and the proton irradiations at a variety of facilities around the world.

July 13, 1995

Dr. Ronald Schrimpf  
1230 E. Speedway, Bldg 104  
Dept. of Electrical & Computer Engineering  
The University of Arizona  
Tucson, AZ 85721

Dear Dr. Schrimpf:

Please accept the enclosed paper, "Single Event Upset and Latchup Measurements in Avionics Devices Using the WNR Neutron Beam and a New Neutron-Induced Latchup Model", for consideration for publication in the Radiation Effects Data Workshop. It was presented at the 1995 IEEE Nuclear and Space Radiation Effects Conference in Madison as part of the Radiation Effects Data Workshop as paper W-3.

Eugene Normand

Boeing Defense & Space Group  
P.O. Box 3999, MS 2T-50  
Seattle, WA 98124  
Phone (206) 544-5626  
FAX (206) 544-5438

Other Boeing Personnel

Jerry L. Wert

Peter P. Majewski

D. L. Oberg

William G. Bartholet

Same Address and FAX as above  
Phone (206) 544-5506  
Phone (206) 544-5390  
Phone (206) 544-5400  
P.O. Box 3999, MS 9F-51  
Phone: (206) 657-6298

Steven A. Wender

Los Alamos National Laboratory  
P-23, MS H803  
Los Alamos, NM 87545  
Phone (505) 667-1344  
FAX (505) 665-4121

Thank you kindly,

Eugene Normand

July 13, 1995

Dr. Ronald Schrimpf  
1230 E. Speedway, Bldg 104  
Dept. of Electrical & Computer Engineering  
The University of Arizona  
Tucson, AZ 85721

Dear Dr. Schrimpf:

Please accept the enclosed paper, "Comparison of Charge Collection Measurements in Silicon and InGaAs Irradiated by Energetic Protons and Neutrons", for consideration for publication in the December 1995 issue of the IEEE Transactions on Nuclear Science. It was presented at the 1995 IEEE Nuclear and Space Radiation Effects Conference in Madison as paper PD-4.

Eugene Normand

Boeing Defense & Space Group  
P.O. Box 3999, MS 2T-50  
Seattle, WA 98124  
Phone (206) 544-5626  
FAX (206) 544-5438

Other Boeing Personnel

Jerry L. Wert

Peter P. Majewski

D. L. Oberg

Same Address and FAX as above

Phone (206) 544-5506

Phone (206) 544-5390

Phone (206) 544-5400

Steven A. Wender

Los Alamos National Laboratory  
P-23, MS H803  
Los Alamos, NM 87545  
Phone (505) 667-1344  
FAX (505) 665-4121

Thank you kindly,

Eugene Normand

July 13, 1995

Dr. Ronald Schrimpf  
1230 E. Speedway, Bldg 104  
Dept. of Electrical & Computer Engineering  
The University of Arizona  
Tucson, AZ 85721

Dear Dr. Schrimpf:

Please accept the enclosed paper, "A New Solar Flare Heavy Ion Model and Its Implementation Through MACREE, An Improved Modeling Tool to Calculate Single Event Effect Rates in Space", for consideration for publication in the December 1995 issue of the IEEE Transactions on Nuclear Science. It was presented at the 1995 IEEE Nuclear and Space Radiation Effects Conference in Madison as paper PH-1.

Peter P. Majewski

Boeing Defense & Space Group  
P.O. Box 3999, MS 2T-50  
Seattle, WA 98124  
Phone (206) 544-5390  
FAX (206) 544-5438

Other Boeing Personnel  
Eugene Normand  
D. L. Oberg

Same Address and FAX as above  
Phone (206) 544-5626  
Phone (206) 544-5400

Thank you kindly,

Eugene Normand